RESEARCH PAPER

Biosynthesized versus Chemically Synthesized Silver Nanoparticles for Acrylic Denture Base Modification: Synthesis, Characterization, and In Vivo Tissue Reaction

Reem A. Hany[1*], Salma Rizk[2], Gihan A. Abdel Rahman[3], Shaymaa I. Habib[4]

[1*]Assistant Lecturer of Dental Materials Science, Dental Biomaterials Department, Faculty of Dentistry, Cairo University; PhD Candidate, Department of Biomaterials, Faculty of Dentistry, Cairo University

Email: Reem.Ahmed@dentistry.cu.edu.eg

[2]Assistant Lecturer of Dental Materials Science, Dental Biomaterials Department, Faculty of Dentistry, MSA University; PhD Candidate, Department of Biomaterials, Faculty of Dentistry, Cairo University

[3]Professor of Dental Materials Science, Biomaterials Department, Faculty of Dentistry, Cairo University

[4]Professor of Dental Materials Science, Biomaterials Department, Faculty of Dentistry, Cairo University

Received: 25th Aug, 2026 | Revised: 1st Sep, 2026 | Accepted: 5th Sep, 2026 | Available Online: 7th Sep, 2026

ABSTRACT

Purpose: This study aimed to evaluate the effect of incorporating silver-nanoparticles (AgNPs) synthesized through biological and chemical routes into acrylic denture-base material on the in-vivo tissue response, compared with unmodified PMMA.

Methods: AgNPs were synthesized using green-tea extract and chemical reduction and characterized by ATR-FTIR, transmission electron microscopy (TEM), and dynamic light scattering (DLS). Fifty-four specimens were allocated to three groups: Group I, biosynthesized AgNPs-modified PMMA (BNS/PMMA); Group II, chemically synthesized AgNPs-modified PMMA (CNS/PMMA); and Group III, unmodified PMMA. For subcutaneous implantation, nine specimens from each group were evaluated at 7 and 14 days. Tissue response was assessed histologically based on inflammatory cell counts and an inflammation scoring system. Statistical significance was set at $p \leq 0.05$.
Results: TEM revealed spherical AgNPs with core diameters 20–30 nm for BNS and 16–20 nm for CNS, without evident agglomeration. DLS showed mean hydrodynamic diameters 51.6 nm and 24.6 nm for BNS and CNS, respectively, with a single predominant peak for each suspension. At 7 days, all groups exhibited moderate inflammation. At 14 days, BNS/PMMA and PMMA showed mild inflammation, whereas CNS/PMMA persisted moderately inflamed. CNS/PMMA exhibited significantly higher inflammatory cell counts than both groups, while no significant difference was observed between BNS/PMMA and PMMA. Inflammatory cell counts decreased significantly from 7 to 14 days in all groups.
Conclusion: Green tea-mediated biological synthesis provided a sustainable alternative to chemical AgNPs synthesis. BNS/PMMA demonstrated favorable tissue response than CNS/PMMA suggesting that AgNPs synthesis route influences the tissue response of modified denture-base materials.

Keywords: Acrylic resin, Denture base, Green synthesis, Green tea, Subcutaneous implantation.

How to cite this article: Reem A. Hany1* Salma Rizk2 Gihan A. Abdel Rahman3 Shaymaa I. Habib4. Biosynthesized versus Chemically Synthesized Silver Nanoparticles for Acrylic Denture Base Modification: Synthesis, Characterization, and In Vivo Tissue Reaction. Int J Drug Deliv Technol. 2026;16(82s):433-435. DOI: 10.25258/ijddt.16.82s.52.

INTRODUCTION

Nanotechnology has become an important area of scientific and technological development, with increasing applications in biomedical and dental materials. Silver nanoparticles (AgNPs) are one of the most attractive nanomaterials because of their broad-spectrum antibacterial, antifungal, antiviral, and anti-inflammatory properties. These characteristics have supported their incorporation into a scale of biomedical purposes, including drug delivery approaches, wound dressings, medical device coatings, and dental materials [(1)].

AgNPs can be synthesized through physical, chemical, or biological approaches. Chemical reduction remains one of the most widely used methods; however, it may involve toxic, corrosive, or environmentally hazardous reducing and stabilizing agents, including sodium borohydride, which can cause skin burns and release flammable gases, and ethylene glycol, which may damage the central nervous system. Such hazards highlight the critical need for safer and more sustainable synthesis strategies [(2)].

In contrast, biological or green synthesis uses naturally derived reducing and capping agents, including plant extracts, proteins, and microorganisms, and has therefore attracted increasing interest as a more sustainable alternative. Plant-mediated synthesis is promising because plants are readily available and contain diverse bioactive compounds, for instance phenolics, flavonoids, terpenoids, polysaccharides, alkaloids, and proteins, which can participate in the reduction of silver ions and stabilization of the resulting nanoparticles [3, 4].

In dentistry, AgNPs have been investigated in several fields, including endodontics, prosthodontics, and implantology, based on their ability to inhibit microbial colonization. However, AgNP toxicity remains a critical concern, primarily attributed to the release of free *Ag*+ ions and the potential for nanoparticles to cross the blood-brain barrier, leading to cerebral accumulation. In-vitro and in-vivo studies have revealed variable biological interactions of AgNPs demonstrating the impact of nanoparticle characteristics and surface chemistry on their performance in biological environments [5].

Polymethyl methacrylate (PMMA) is the standard dental polymer for denture bases, yet its rough surfaces combined with poor oral hygiene and xerostomia, frequently lead to denture stomatitis. Accordingly, incorporation of AgNPs into denture base polymers has been proposed as a strategy to impart antimicrobial properties. Although AgNP incorporation has been investigated as a strategy to improve the antimicrobial properties of denture base resins, limited information is available regarding whether AgNPs produced through different synthesis approaches elicit different biological responses after incorporation into PMMA. Since the synthesis route can influence the physicochemical and surface characteristics of AgNPs and consequently their interactions with biological tissues, direct comparison of biosynthesized and chemically synthesized AgNPs incorporated into denture base materials is required [6].

Therefore, this study aimed to prepare and characterize AgNPs using biological and chemical approaches and to compare the in vivo tissue response of acrylic denture bases modified with the resulting nanoparticle preparations, with unmodified conventional acrylic denture base material serving as the control.

The null hypothesis was that there would be no significant difference in the in-vivo tissue response among acrylic denture base materials modified with biosynthesized AgNPs, chemically synthesized AgNPs, and unmodified conventional acrylic denture base material.

MATERIALS AND METHODS

I. Preparation of Silver Nanoparticle Suspensions

a. Biologically Synthesized Silver Nanoparticle Suspension Using Green Tea Extract

Green tea (GT) extract was prepared by dissolving 10 g of commercial green tea powder (Imtenan Company, Egypt) in 500 mL of distilled water, stirred at 60 °C for 10 min, and left to cool to room temperature (~25 °C) over 6 h. The extract was then filtered to remove particulate matter, and the resulting clear filtrate was used immediately for AgNPs synthesis.

For biosynthesis, 50 mL of the freshly prepared GT extract was transferred to an Erlenmeyer flask, placed in an ice bath, and continuously stirred. Subsequently, 5 mL of 10 mM silver nitrate ($AgNO_3$, Merk, Germany) was added dropwise under continuous stirring, resulting in a final Ag nanoparticles concentration of approximately 1 mM. The phytochemicals present in the GT extract acted as reducing and stabilizing agents, promoting the reduction of Ag^+ ions and formation of biosynthesized AgNPs (BNS) [7].

b. Chemically Synthesized Silver Nanoparticles Liquid Suspension

Chemically synthesized AgNPs (CNS) were prepared via reduction with sodium borohydride ($NaBH_4$) (Research Lab, India) using polyvinyl pyrrolidone (PVP) (Merk, Germany) as a capping agent. First, 50 mL of 0.01 M $NaBH_4$ was placed in an Erlenmeyer flask in an ice bath and stirred for 20 min. Then, 2 mL of 0.025 M $AgNO_3$ containing 1% PVP was added dropwise. The ice bath was essential to moderate the strong reducing action of $NaBH_4$, thereby slowing nucleation/growth and improving particle size and shape uniformity. A color shift from light to brighter yellow confirmed AgNP formation. The resulting PVP-stabilized, monodispersed AgNPs had a final concentration of 1 mM [8]. A schematic illustration of green tea extraction steps with the biosynthesis and chemical synthesis of AgNPs is shown in figure (1).

The working concentrations of the two AgNPs suspensions were selected during formulation optimization following preliminary evaluation of their antifungal activity against *Candida albicans*. Accordingly, the biosynthesized AgNPs suspension was diluted 1:1 with distilled water, whereas the chemically synthesized AgNPs suspension was used at its original concentration. These respective working formulations were then incorporated into the acrylic denture base material using the same incorporation protocol.

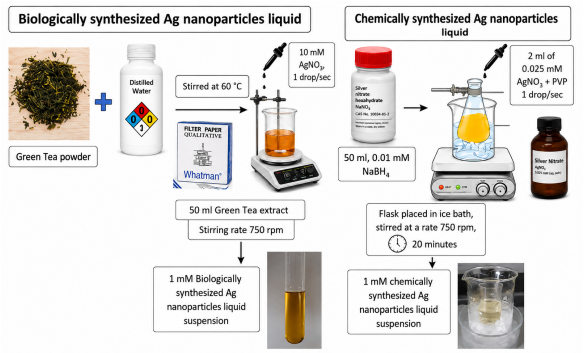

Figure (1): Steps of green tea extraction and synthesis of AgNPs via biological and chemical routes.

II. Characterization of Silver Nanoparticle Suspensions

Fourier Transform Infrared Spectroscopy (FTIR):

FTIR analysis was performed to identify the functional groups associated with the green tea extract and the surface chemistry of the biosynthesized and chemically synthesized AgNPs. Spectra were acquired 24 h after preparation using an FTIR-ATR spectrometer (Vertex 70-RAM II, Bruker, Germany) over the range of 400–4000 cm^{-1} in transmittance mode at room temperature. For analysis, 100 µL of each sample was directly applied to the ATR crystal without prior sample preparation [9].

Transmission Electron Microscopy (TEM):

The morphology and metallic core size of the synthesized AgNPs were examined using high-resolution transmission electron microscopy operated at an accelerating voltage of 200 kV (HR-TEM, JEOL JEM-2100, Japan). A 10 µL aliquot of each AgNP suspension was deposited onto a 300-mesh Formvar/carbon-coated copper grid and allowed to air-dry at room temperature. Transmission electron micrographs were then analyzed using imaging software [9].

Dynamic Light Scattering (DLS)

The hydrodynamic diameter and particle size distribution of the synthesized AgNPs were determined by dynamic light scattering using a Zetasizer Nano ZS90 (Malvern Panalytical, UK) at a fixed backscattering angle of 173° and a temperature of 25 °C. The hydrodynamic diameter reflects the effective particle size in suspension, including any coating, stabilizing or capping layer. The polydispersity index (PdI) was recorded as an indicator of the particle size distribution homogeneity. For analysis, 1 mL of each AgNP suspension was diluted with 9 mL of distilled water and sonicated for 10 min to minimize particle aggregation. Measurements were performed in triplicate [9].

III. Preparation Of Acrylic Denture Base Specimens

In the current study, the acrylic denture base specimens were allocated into three groups according to the type of AgNP suspension incorporated into the PMMA resin: **Group I**, biosynthesized AgNP-modified PMMA (BNS/PMMA); **Group II**, chemically synthesized AgNP-modified PMMA (CNS/PMMA); and **Group III**, unmodified conventional PMMA (control group).

A standardized preparation protocol, based on the method reported by Sun et al. (2021) [10], with modifications, was used to prepare the AgNP-modified acrylic denture base specimens. The same incorporation procedure was applied to both experimental groups to ensure consistency of AgNPs incorporation and minimize variability in nanoparticles dispersion within the PMMA matrix.

For the experimental groups, the respective AgNP suspension (biosynthesized AgNPs for Group I [BNS/PMMA] or chemically synthesized AgNPs for Group II [CNS/PMMA]) was first mixed with acrylic acid, used as a coupling agent, at a 1:3 volume ratio. The resulting mixture was then incorporated into the MMA monomer (Implacryl, Vertex-Dental B.V., Netherlands) at a 1:3 volume ratio and mixed to obtain a homogeneous liquid phase. PMMA powder was subsequently added to the modified liquid phase at a powder to liquid volume ratio of 2:1, following the manufacturer's recommended ratio. The resulting dough was manipulated and processed according to the manufacturer's instructions to obtain the required specimens [10].

For the conventional acrylic denture base control group (Group III; PMMA), PMMA powder was directly mixed with MMA monomer at the manufacturer's recommended powder-to-liquid volume ratio of 2:1. The mixture was subsequently manipulated and processed in accordance with the manufacturer's instructions using the same specimen preparation and processing conditions as those applied to the experimental groups [10]. Disc-shaped specimens (4 mm diameter x 2 mm thickness) were fabricated using split Teflon molds. The specimens were processed using the conventional flasking and compression molding technique and polymerized according to a heat-curing cycle of 70 °C for 90 min followed by 100 °C for 30 min. After completion of the curing cycle, the specimens were allowed to bench-cool to room temperature, deflasked, finished, and polished under standardized conditions. The specimens were subsequently sterilized by autoclaving prior to subcutaneous implantation.

IV. In Vivo Evaluation of Tissue Reaction:

a. Animal Model:

The sample size was calculated using G*Power software, Version 3.1.9.7 (Heinrich-Heine-Universität Düsseldorf, Germany). Based on an effect size (f) of 0.40 derived from a previous study (11), with a 5 % significance level, 80% statistical power, and a 0.50

correlation among repeated measures, the minimum required sample size was 51 specimens. This was increased to 54 specimens to ensure equal allocation, resulting in 9 specimens per group at each implantation interval (7 and 14 days).

Eighteen adult male Wistar rats (200–250 g; approximately 6 months old) were used and equally allocated to two implantation periods (7 and 14 days; n = 9 rats/time point). Each rat received one specimen from each material group, resulting in three implanted specimens per animal. The rats were maintained in a temperature-controlled room and received food and water *ad libitum*. The test was conducted after taking the approval of the ethics committee on animal use (IACUC, approval CU-III-F-77-22).

b. Subcutaneous Implantation and Histological Analysis:

Following Sun et al. (2021) [10], anesthesia was induced with ketamine (Hikma Pharma, UK, 25 mg/kg) and xylazine (Bimeda USA, 10 mg/kg). The dorsal skin was shaved, disinfected, and three longitudinal 4-mm incisions were made to create three subcutaneous pockets (3 cm apart) by blunt dissection. One specimen from each group was implanted in a separate pocket, and incisions were closed with 4-0 silk sutures. After 7 and 14 days, the rats were euthanized with sodium pentobarbital overdose (150 mg/kg). The implantation sites were examined macroscopically for erythema and edema, after which the specimens with surrounding tissues were excised and fixed in 10% neutral-buffered formalin (Sigma-Aldrich, Merck, Germany) for 24 h. For histopathology, specimens were gently removed, and tissue sections of 3 µm thickness were prepared and stained with H&E (Sigma-Aldrich, Merck, Germany). The inflammatory response was scored from 0 to 3 according to the number of inflammatory cells per high-power field: 0 (absent), 1 (<25 cells), 2 (25–124), or 3 (≥125 cells) [12]. Mean cell counts were determined in three separate areas of each histological section at ×400 magnification. All counts were performed by a single blinded evaluator to ensure consistency. Representative photomicrographs for each group were subsequently captured at ×100 magnification [10].

V. Statistical Analysis:

Data were analyzed using MedCalc Statistical Software, version 22 for Windows (MedCalc Software Ltd, Ostend, Belgium). Continuous data were explored for normality using Kolmogrov Smirnov test and Shapiro Wilk test and expressed as mean and standard deviation. Repeated-measures ANOVA with Bonferroni-adjusted pairwise comparisons were used for intergroup comparisons, while paired *t*-test was used for intragroup comparisons. Categorical data were expressed as frequency and percentage, analyzed using Cochran's Q test followed by multiple comparisons, and McNemar's test for intragroup comparisons. Statistical significance was set at $P \leq 0.05$, with Bonferroni-corrected comparisons at $P \leq 0.016$. All tests were two-tailed with 95% confidence intervals and 80% statistical power.

RESULTS:

Characterization Of Silver Nanoparticle Suspensions:

- **Fourier Transform Infrared Spectroscopy (FTIR):**

The FTIR spectra of green tea extract (GTE) and the prepared AgNP suspensions are shown in figure (2). FTIR spectrum of the green tea extract revealed several characteristic absorption bands associated with its phytochemical constituents. A strong broad peak at 3295 cm^{-1} was attributed mainly to O–H stretching, while the band at 2927 cm^{-1} corresponded to aliphatic C–H stretching. The bands observed at 1693 and 1606 cm^{-1} were associated with carbonyl and aromatic C=C stretching, respectively, whereas the bands at 1555 and 1517 cm^{-1} were related to N–H/C–N and aromatic vibrations. A prominent band at 1031 cm^{-1} was attributed mainly to C–O–C stretching. These overall bands confirmed the presence of hydroxyl-, carbonyl-, aromatic-, and carbohydrate-associated functional groups in the green tea extract, which may participate in the reduction and stabilization of AgNPs [13-15].

The FTIR spectrum of the biosynthesized AgNPs exhibited characteristic bands at 3323, 2973, 2883, 1379, 1087, 1045, 879, and 667 cm^{-1}, with an additional band at 430 cm^{-1}. Compared with the spectrum of the green tea extract, changes in band positions and intensities were observed following AgNP synthesis, particularly in the O–H-, C–H-, and C–O-associated regions. These spectral changes suggest the involvement of phytochemical functional groups in the reduction and surface stabilization of the biosynthesized AgNPs [16-19].

In contrast, the chemically synthesized AgNPs exhibited characteristic bands at 2951, 1646, 1493, 1460, 1421, 1285, 841, and 646 cm^{-1}, with an additional band at 571 cm^{-1}. The prominent band at 1646 cm^{-1} was associated with the carbonyl group of PVP, while the changes in the characteristic PVP bands suggest its interaction with and stabilization of the AgNP surface. The differences in the FTIR profiles of the two AgNP preparations indicate distinct surface chemistry associated with their respective reducing and capping systems [16-19].

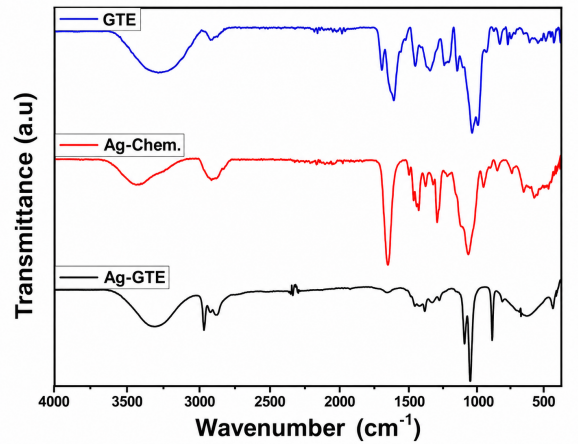

Figure (2): The FTIR spectra of green tea extract, chemically synthesized AgNPs, and biologically synthesized AgNPs

- **Transmission Electron Microscopy (TEM):**

TE micrographs revealed predominantly spherical, monodispersed AgNPs with no evident agglomeration, with core diameters ranging from 20–30 nm for the biosynthesized AgNPs and 16–20 nm for the chemically synthesized AgNPs , Figure (3).

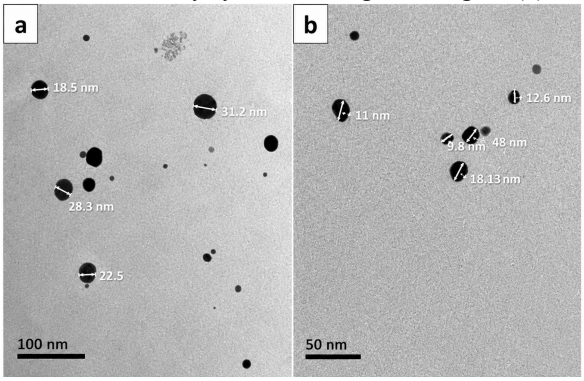

Figure (3): TE micrographs of (a) biosynthesized and (b) chemically synthesized AgNPs suspensions. Scale bars: 100 nm and 50 nm, respectively.

Dynamic Light Scattering:

Dynamic light scattering (DLS) analysis of the biosynthesized AgNP suspension revealed a mean hydrodynamic diameter of 51.6 nm with a PdI of 0.29, indicating a relatively narrow particle-size distribution. A single predominant peak was observed in the particle-size distribution profile. The chemically synthesized AgNP suspension showed a smaller mean hydrodynamic diameter of 24.6 nm, with a PdI of 0.41, indicating a broader size distribution compared with the biosynthesized AgNPs. The corresponding distribution profile showed a single predominant peak, Figure (4).

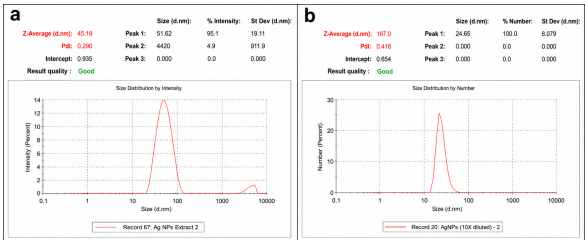

Figure (4): The hydrodynamic size distribution of (a): biologically synthesized AgNPs and (b) chemically synthesized AgNPs, determined by DLS.

In Vivo Tissue Reaction Results:

No apparent systemic adverse effects were observed during the experimental period. Macroscopic visual examination of the implantation sites revealed complete wound healing by day 7, with no evident erythema, edema, necrosis, or granuloma formation in any group at either implantation interval. Mean and standard deviation values for the inflammatory cell counts are presented in Table (1) and Figure (5). Significant differences among the groups were observed at both 7 and 14 days ($P < 0.001$). The CNS/PMMA group showed significantly higher inflammatory cell counts than both the BNS/PMMA and PMMA groups, whereas no significant difference was observed between BNS/PMMA and PMMA ($P > 0.05$). In all groups, inflammatory cell counts decreased significantly from 7 to 14 days ($P < 0.05$).

The distribution of inflammation scores is presented in Table (2). At 7 days, all groups exhibited moderate inflammation, with no significant intergroup difference ($P = 1.000$). At 14 days, a significant intergroup difference was observed ($P=0.002$), with milder inflammation predominating in the BNS/PMMA and PMMA groups, whereas the CNS/PMMA group remained moderately inflamed. Intragroup analysis demonstrated a significant reduction in inflammation scores from 7 to 14 days for BNS/PMMA and PMMA, but not for CNS/PMMA.

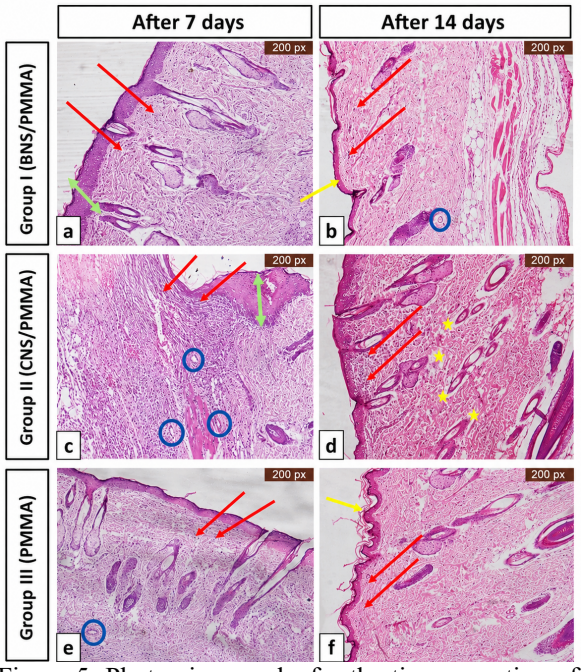

Figure 5: Photomicrographs for the tissue reaction of the different groups after 7 and 14 days of implantation. (a): BNS/PMMA samples after 7 days showing thickened stratified squamous epithelium (green arrow) and moderate number of inflammatory cells (red arrows, purple dots), **b:** BNS/PMMA samples after 14 days showing thin stratified squamous epithelium and mild inflammation cells (red arrows), **c:** CNS/PMMA samples after 7 days showing hyperplastic stratified squamous epithelium (green arrow), dilated blood capillaries with RBCs (blue circles) and moderate inflammation cells (red arrows), **d:** CNS/PMMA samples after 14 days presenting a persistent moderate inflammatory cell infiltration (red arrows) and pale areas of mild oedema (yellow stars), **e:** PMMA samples after 7 days showing moderate inflammatory response and dilated blood capillaries (blue circle), **f:** PMMA samples after 14 days showing a thin stratified squamous epithelium and shift to mild inflammatory response, (H&E x100).

Table (1): Mean and Standard Deviation of Number of Inflammatory Cells In Each Group Showing The Effect of Groups and Time Intervals:

	Group I (BNS/PMMA)		Group II (CNS/PMMA)		Group III (PMMA)		P value
	Mean	**SD**	**Mean**	**SD**	**Mean**	**SD**	
7 days	42.55 Ba	12.62	65.77 Aa	14.52	37.33 Ba	11.76	P < 0.001*
14 days	22.66 Bb	5.72	34.44 Ab	8.23	20.44 Bb	3.50	P < 0.001*
P value	P = 0.0025*		P = 0.0002*		P = 0.0021*		

Superscripts with different capital letters indicate statistically significant difference within the same row. Superscripts with different small letters indicate statistically significant difference within the same column.

* Corresponds to statistically significant ($p \leq 0.05$), ns; non-significant ($p > 0.05$).

Table (2): Frequency and Percentage of Scores of Inflammations in Each Group Showing The Effect of Groups and Time Intervals:

	Group I (BNS/PMMA)		Group II (CNS/PMMA)		Group III (PMMA)		**P value**
	Mild	Moderate	Mild	Moderate	Mild	Moderate	
7 days	0(0%)	9(100%)	0(0%)	9(100%)	0(0%)	9(100%)	P = 1.000
14 days	6(66%)	3(33%)	0(0%)	9(100%)	8(88%)	1(11%)	P =

da ys	.7%)	.3%)	0 %)	0%)	.9%)	.1%)	0.0 02 *
P va lu e	P = 0.0313*		P = 1.0000		P = 0.0078*		

* Corresponds to statistically significant ($p \leq 0.05$).

DISCUSSION:

The current study was designed to evaluate the tissue reaction of acrylic denture bases modified with silver nanoparticles (AgNPs) synthesized through two different routes: a sustainable biological method using green tea extract and a traditional chemical reduction method. The study was designed to determine whether the synthesis route influences the tissue response to AgNP-modified PMMA, with unmodified conventional PMMA serving as the control. Silver nanoparticles (AgNPs) have gained great attention in dental and biomedical applications owing to their distinctive physical and bio-chemical properties and broad antimicrobial potential, in contrast with their macro and micro complements. However, their biological behavior may be influenced by the synthesis route, which can affect nanoparticle characteristics, surface chemistry, and the nature of the associated reducing and capping agents. Therefore, comparing AgNPs produced by different synthesis approaches is important when considering their incorporation into materials intended for direct contact with biological tissues.

For the biologically synthesized silver nanoparticles (BNS), green tea (GT) extract served as both a reducing and capping agent, utilizing its rich array of bioactive agents like polyphenols and catechins to drive the reduction of silver ions. In contrast, the chemically synthesized silver nanoparticles (CNS) were produced via reduction with sodium borohydride ($NaBH_4$), with polyvinyl pyrrolidone (PVP) added as a capping agent to ensure particle stability [20].

FTIR characterization provided insight into the surface chemistry and functional groups of the biosynthesized AgNPs and the potential involvement of green tea phytochemicals in their formation and stabilization. The spectrum of the biosynthesized AgNP suspension retained several characteristic bands of the green tea extract, with changes in their position and/or intensity following nanoparticle synthesis. The broad O–H stretching band at 3323 cm^{-1} is consistent with hydroxyl-containing polyphenolic constituents, including catechins, while the bands at 879 and 667 cm^{-1} can be associated with aromatic and flavonoid-related vibrations. The retention and modification of these bands following synthesis suggests the involvement of phytochemical functional groups in the reduction and surface stabilization of the AgNPs. A low-intensity band at 430 cm^{-1} was also observed, consistent with Ag-related vibrations. Similar FTIR profiles and the involvement of plant-derived functional groups in the synthesis and stabilization of green-synthesized AgNPs have been reported previously [19, 21-25].

In the chemically synthesized AgNP suspension, the weak aliphatic C–H stretching band at 2951 cm^{-1} is characteristic for vinyl polymer backbone (–CH_2–CH–) of the polymer chain, confirming the presence of PVP. The shift of the carbonyl (C=O) band from 1665 to 1640 cm^{-1} indicates electron donation from PVP's carbonyl oxygen to Ag^+/AgNPs, forming a protective layer and supporting the role of PVP in nanoparticle stabilization. A weak band at 571 cm^{-1} was also observed, which has previously been associated with Ag-related vibrations. Similar FTIR features have been reported for PVP-capped chemically synthesized AgNPs [16-19, 26-28].

TEM and DLS provided complementary information regarding the morphology and size characteristics of the synthesized AgNPs. TE micrographs revealed predominantly spherical particles with no evident agglomeration [8, 9], while DLS demonstrated a single predominant peak for both suspensions, indicating relatively narrow hydrodynamic size distributions. The mean hydrodynamic diameter was higher for the biosynthesized AgNPs (51.6 nm) than for the chemically synthesized AgNPs (24.6 nm), despite their comparable smaller core sizes observed by TEM. This difference may be attributed to the organic phytochemical layer associated with the biosynthesized nanoparticles, which contributes to their hydrodynamic diameter, whereas the chemically synthesized particles were capped with PVP. The PdI values of 0.29 and 0.41 for the biosynthesized and chemically synthesized AgNPs, respectively, indicated relatively narrow to moderate particle-size distributions [29, 30]. The observed morphological and size characteristics align with the work of Ajitha et al. (2015) [9] and Widatalla et al. (2022) [8]

Regarding the tissue reaction following subcutaneous implantation, all groups initially showed moderate inflammation at 7 days. By 14 days, the BNS/PMMA and conventional PMMA groups showed a shift toward mild inflammation, whereas the CNS/PMMA group remained within the moderate category. The reduction in inflammatory response over time is consistent with the transient tissue reaction associated with surgical

trauma and implantation of acrylic resin materials. Residual MMA monomer may also contribute to the early inflammatory response following polymerization, with progressive diffusion and reduction of the local irritant stimulus potentially contributing to resolution over time [31, 32].

The comparatively lower inflammatory response observed with BNS/PMMA may be related to differences in the chemical environment associated with the two synthesis routes. Chemical reduction commonly involves strong reducing and stabilizing agents, and residual reaction products may influence the biological response if retained within the nanoparticle preparation. In the present study, sodium borohydride was used as the reducing agent for CNS synthesis. Sodium Borohydride does not disappear; it gets oxidized giving primary by-products like Borate/Boric Acid which is the most likely reason for irritation. Borate ions are biologically active and can be cytotoxic at high concentrations, where they can interfere with cellular metabolism and enzyme function. Even at low concentrations, residual borates are known to cause irritation to tissues and can provoke a local inflammatory response. In a subcutaneous implant, where the clearance is slow, these ions can leach out continuously, maintaining a state of irritation [33]. In contrast, the biological synthesis route uses green tea phytochemicals as reducing and capping agents, resulting in a nanoparticle surface associated with naturally derived compounds. These phytochemicals, including polyphenolic constituents and catechins, possess reported antioxidant and anti-inflammatory properties, which may contribute to the more favorable tissue response observed with BNS/PMMA [34, 35]. Therefore, not only there are fewer toxic chemical residuals, but the capping layer itself may actually suppress the inflammatory response that the body would normally display.

The significant reduction in inflammatory cell counts from 7 to 14 days in all groups is consistent with the expected progression of the local tissue response following implantation. This could be because immediately after implantation, the surgical trauma and the presence of a foreign body trigger the acute inflammatory response. The body rapidly recruits a large number of neutrophils and macrophages to the site as a defensive and clean-up operation [36]. So, the high inflammatory cell count at 7 days represents the peak of this acute phase. As tissue healing progresses and the acute stimulus subsides, the inflammatory response generally decreases, resulting in fewer inflammatory cells at the implantation site, which was observed at day 14. The absence of necrosis or other severe tissue alterations further supports the resolution of the local inflammatory response over time [37].

Based on the current study results, the null hypothesis was partially rejected, as a significant difference in tissue response was observed between the chemically synthesized AgNPs-modified group and the other groups, whereas no significant difference was found between the biosynthesized AgNPs-modified and conventional PMMA groups.

CONCLUSIONS

Green tea-mediated biological synthesis provided a sustainable alternative to chemical reduction, with BNS-modified PMMA showing a more favorable tissue response than CNS-modified PMMA and a response comparable to unmodified PMMA. These findings suggest that the AgNPs synthesis route influences the tissue response of modified denture base materials.

ACKNOWLEDGMENTS

Not applicable

AUTHORS' CONTRIBUTION

All authors contributed to the study design. Conceptualisation: G.A.R and S.I.H. Data acquisition: R.A.H and S.K.R. Data analysis and interpretation: R.A.H. Investigation: R.A.H and S.K.R. Supervision: G.A.R and S.I.H. Validation: G.A.R and S.I.H. Visualization: G.A.R and S.I.H. Writing original draft: R.A.H. Writing review and editing: R.A.H, G.A.R and S.I.H.

FUNDING

No funding was received for this work.

AVAILABILITY OF DATA AND MATERIALS

The datasets used and/or analyzed during the current study are available from the corresponding author upon reasonable request.

DECLARATIONS

ETHICS APPROVAL AND CONSENT TO PARTICIPATE

The followed animal protocol was approved by the CU-IACUC reviewers. Approval number: CU-III-F-77-22

CONSENT FOR PUBLICATION

Not applicable.

COMPETING INTERESTS

The authors declare that they have no competing interests.

REFERENCES

1. Nanosilver E. State of the Science Literature Review: Everything Nanosilver and More.
2. Kaur P, Luthra R. Silver nanoparticles in dentistry: An emerging trend. SRM Journal of Research in Dental Sciences. 2016;7(3):162.
3. León-Silva S, Fernández-Luqueño F, López-Valdez F. Silver nanoparticles (AgNP) in the

environment: a review of potential risks on human and environmental health. Water, Air, & Soil Pollution. 2016;227(9):1-20.
4. Park E-J, Yi J, Kim Y, Choi K, Park K. Silver nanoparticles induce cytotoxicity by a Trojan-horse type mechanism. Toxicology in vitro. 2010;24(3):872-8.
5. Corrêa JM, Mori M, Sanches HL, Cruz ADd, Poiate E, Poiate IAVP. Silver nanoparticles in dental biomaterials. International journal of biomaterials. 2015;2015.
6. Prokopovich P, Köbrick M, Brousseau E, Perni S. Potent antimicrobial activity of bone cement encapsulating silver nanoparticles capped with oleic acid. Journal of Biomedical Materials Research Part B: Applied Biomaterials. 2015;103(2):273-81.
7. Krithiga N, Rajalakshmi A, Jayachitra A. Green synthesis of silver nanoparticles using leaf extracts of Clitoria ternatea and Solanum nigrum and study of its antibacterial effect against common nosocomial pathogens. Journal of Nanoscience. 2015;2015.
8. Widatalla HA, Yassin LF, Alrasheid AA, Ahmed SAR, Widdatallah MO, Eltilib SH, et al. Green synthesis of silver nanoparticles using green tea leaf extract, characterization and evaluation of antimicrobial activity. Nanoscale Advances. 2022;4(3):911-5.
9. Ajitha B, Ashok Kumar Reddy Y, Sreedhara Reddy P. Green synthesis and characterization of silver nanoparticles using Lantana camara leaf extract. Mater Sci Eng C Mater Biol Appl. 2015;49:373-81.
10. Sun J, Wang L, Wang J, Li Y, Zhou X, Guo X, et al. Characterization and evaluation of a novel silver nanoparticles-loaded polymethyl methacrylate denture base: In vitro and in vivo animal study. Dent Mater J. 2021;40(5):1100-8.
11. Radhi AA, Hashim AF, Ghani T. Histopathological picture of heat cured acrylic resin modified with nano-composite filler (in vivo study). Health. 2020;23(S6):671.
12. Karanth P, Manjunath M, Kuriakose E. Reaction of rat subcutaneous tissue to mineral trioxide aggregate and Portland cement: a secondary level biocompatibility test. Journal of Indian Society of Pedodontics and Preventive Dentistry. 2013;31(2):74.
13. Bisht K, Pandey N, Gautam S, Lohani P. Determination of Polyphenols, reducing potential and FT-IR analysis of green tea (Camellia sinensis L.) leaves extract for nanoparticles synthesis. Journal of Advances in Biology & Biotechnology. 2024;27(8):842-50.
14. Parvez S, Wani IA. Comparative Study of Composition and Antioxidant Properties of Green Tea Extracts from Different Commercial Grades. ACS Food Science & Technology. 2025;5(4):1678-86.
15. Giorgini E, Notarstefano V, Foligni R, Carloni P, Damiani E. First ATR-FTIR characterization of black, green and white teas (Camellia sinensis) from European tea gardens: a PCA analysis to differentiate leaves from the in-cup infusion. Foods. 2023;13(1):109.
16. Franca T, Goncalves D, Cena C. ATR-FTIR spectroscopy combined with machine learning for classification of PVA/PVP blends in low concentration. Vibrational Spectroscopy. 2022;120:103378.
17. ALjubouri F, Jawad MK. FTIR and electrical behavior of blend electrolytes based on (PVA/PVP). Iraqi Journal of Physics. 2023;21(1):1-9.
18. El-Shamy OA, Deyab M. Novel anticorrosive coatings based on nanocomposites of epoxy, chitosan, and silver. Materials Letters. 2023;330:133298.
19. El-Shamy OA, El-Adawy MM, Abdelsalam M. Chemical synthesis of a polyvinylpyrrolidone-capped silver nanoparticle and its antimicrobial activity against two multidrug-ResistantAeromonas species. Aquaculture Research. 2023;(1):3641173.
20. Barbir D, Dabić P, Weber I, Rakić A. Green Synthesis of Silver Nanoparticles Using Green Tea: Characterisation and Antibacterial Properties. Kemija u Industriji. 2025;74.
21. Safa MAT, Koohestani H. Green synthesis of silver nanoparticles with green tea extract from silver recycling of radiographic films. Results in Engineering. 2024;21:101808.
22. Loo YY, Chieng BW, Nishibuchi M, Radu S. Synthesis of silver nanoparticles by using tea leaf extract from Camellia sinensis. International journal of nanomedicine. 2012:4263-7.
23. Rolim WR, Pelegrino MT, de Araújo Lima B, Ferraz LS, Costa FN, Bernardes JS, et al. Green tea extract mediated biogenic synthesis of silver nanoparticles: Characterization, cytotoxicity evaluation and antibacterial activity. Applied Surface Science. 2019;463:66-74.
24. Hermanto D, Ismillayli N, Irmawanti I, Fathulloh I, Nila D, Zuryati UK, et al.

Electrochemically synthesized biogenic silver nanoparticles using green tea extract as a promising antioxidant. Karbala International Journal of Modern Science. 2023;9(1):8.
25. Hasan WL, Sari R, Hendradi E. Green synthesis of antimicrobial silver nanoparticles using green tea extract: The role of concentration and pH. Jurnal Sains Farmasi & Klinis. 2024;11(1):25-31.
26. Chahar V, Sharma B, Shukla G, Srivastava A, Bhatnagar A. Study of antimicrobial activity of silver nanoparticles synthesized using green and chemical approach. Colloids and Surfaces A: Physicochemical and Engineering Aspects. 2018;554:149-55.
27. Rajanandkumar R. Synthesis and characterization of polymer encapsulated silver nanoparticle coatings for antibacterial effect. Materials Today: Proceedings. 2021;47:1782-6.
28. Dinesh B, Poyya J, Zameer F, Sannegowda LK, Joshi CG, Raghu AV. Effect of polyvinylpyrrolidone on antioxidant and antibacterial activity of silver metal nanoparticles: a comparative analysis. Proceedings of the National Academy of Sciences, India Section A: Physical Sciences. 2024;94(4):359-68.
29. Dayana BM, Venkatesan R, Joseph Prakash JT, Saravanan P, Nivetha MS, Murali A, et al. Biosynthesis of silver nanoparticles via Melaleuca alternifolia leaf extract for antibacterial, antifungal, antioxidant and anticancer activity. Sci Rep. 2026;16(1):2574.
30. Jemel I, Krayem N, Jlidi H, Ben Bacha A, Alonazi M, Charguia R, et al. Structural insights and biomedical potential of biosynthesized silver nanoparticles: antibacterial activity, anti-biofilm and cancer cell inhibition. PeerJ. 2025;13:e19608.
31. Jorge JH, Giampaolo ET, Machado AL, Vergani CE. Cytotoxicity of denture base acrylic resins: a literature review. The Journal of prosthetic dentistry. 2003;90(2):190-3.
32. Gajewski VE, Pfeifer CS, Fróes-Salgado NR, Boaro LC, Braga RR. Monomers used in resin composites: degree of conversion, mechanical properties and water sorption/solubility. Brazilian dental journal. 2012;23:508-14.
33. Yunusoglu O, Kalfa I, Demirel M, Binzet M, Sevinc U, Turel I, et al. A comprehensive review of the pharmacological, therapeutic, and toxicological properties of boric acid and other boron-containing compounds: current landscape and future perspectives.
34. Al-Sheddi ES, Farshori NN, Al-Oqail MM, Al-Massarani SM, Saquib Q, Wahab R, et al. Anticancer potential of green synthesized silver nanoparticles using extract of Nepeta deflersiana against human cervical cancer cells (HeLA). Bioinorganic Chemistry and Applications. 2018;2018(1):9390784.
35. Al-Ghamdi S, Alkathiri T, Alfarraj A, Alatawi OM, Alkathiri A, Panneerselvam C, et al. Green synthesis and characterization of zinc oxide nanoparticles using Camellia sinensis tea leaf extract and their antioxidant, anti-bactericidal and anticancer efficacy. Research on Chemical Intermediates. 2022;48(11):4769-83.
36. da Silva EV, Goiato MC, Bitencourt SB, Brito VG, Takamyia AS, Penitente PA, et al. Evaluation of Different Polymerisation Methods of Ocular Prosthesis Acrylic Resins on Subcutaneous Tissue Inflammatory Response in Rats. Sultan Qaboos University Medical Journal. 2022;22(2):233.
37. Anderson JM, Rodriguez A, Chang DT, editors. Foreign body reaction to biomaterials. Seminars in immunology; 2008: Elsevier.